Journal of Asian Concrete Federation
Vol. 11, No. 1, pp. 1-14, March 2025
ISSN 2465-7964/ eISSN 2465-7972
DOI http://dx.doi.org/10.18702/acf.2024.11.1.1

**Technical Paper**

# Simulation of Concrete DEF Expansion Under Restraint Using 3D RBSM

**Jie Luo, Shingo Asamoto, Kohei Nagai***

(Received: 13-Jan-2025; Revised: 10-Feb-2025; Accepted: 02-Mar-2025; Published online: 20-Mar-2025)

**Abstract**: Delayed ettringite formation (DEF) is a durability issue that can cause concrete expansion and cracking. While significant efforts have been made to investigate the microscopic mechanisms of DEF expansion, relatively few studies have focused on structural models. Understanding the effect of stress on DEF expansion is crucial for evaluating the performance of structures affected by this phenomenon. Although experiments are useful for studying structural performance under certain conditions, visualizing the internal state of concrete and reinforcement through experiments is challenging. Therefore, numerical simulation is generally a more effective method for making such predictions. In this study, the discrete numerical analysis method, 3D Rigid Body Spring Model (RBSM), is used to simulate concrete DEF expansion under external restraint. The simulation is based on one experiment, and it discusses the macroscopic expansion and anisotropic expansion behavior due to restraint. Both the surface cracking pattern and the internal crack development are visualized through the simulation. The reasonableness of the simulation results and the limitations of RBSM in simulating DEF under restraint conditions are discussed in this paper, which enables further study of DEF damage at the structural level using this simulation method.

**Keywords**: Delayed ettringite formation (DEF), external restraint, cracking development, 3D RBSM

## 1. Introduction

Delayed ettringite formation (DEF) is a durability issue that can lead to concrete expansion and cracking. While similar cracking and expansion phenomena have been observed in reinforced concrete (RC) structures affected by alkali-silica reaction (ASR) and DEF [1–4], the underlying mechanisms of damage in these two cases are fundamentally different. DEF-induced expansion is typically more severe than ASR-induced expansion in terms of magnitude. While considerable effort has been made to investigate the microscopic mechanisms of DEF expansion [5–7], relatively few studies have focused on structural models [3,8,9]. Understanding the effect of stress on DEF expansion is crucial for evaluating the performance of structures affected by this phenomenon.

Several studies have examined ASR expansion under stress [10–20], reporting that the presence of steel reinforcement and stresses, such as prestressing, reduces expansion in both the restrained and loaded directions. Multon and Toutlemonde [11] highlighted that the expansion shifts to the direction with less compression, leading to nearly equal volumetric expansion, a phenomenon termed "expansion transfer." However, in concrete or mortar undergoing DEF expansion, stress reduces expansion in the restrained direction without a corresponding increase in the unrestrained direction, indicating an absence of expansion transfer [11,21,22]. This results in a reduced volumetric expansion of concrete under uniaxial restraint (20–33%) [21,23]. Notably, when concrete is triaxially reinforced, volumetric expansion decreases significantly to 54% of free expansion [23]. The differences between ASR and DEF stem from the varying viscosities of the chemical products formed during these reactions. ASR

*Corresponding author **Kohei Nagai** *is a professor of the Graduate School of Engineering, Hokkaido University, Hokkaido, Japan. Email: nagai325@ eng.hokudai.ac.jp*
**Jie Luo** *is a postdoctoral researcher of the Graduate School of Engineering, Hokkaido University, Hokkaido, Japan. Email: luojie@eng. hokudai.ac.jp*
**Shingo Asamoto** *is an associate professor of Department of Civil and Environmental Engineering, Saitama University, Saitama, Japan. Email: asamoto@mail.saitama−u.ac.jp*

products, being more mobile, can migrate through pores and cracks, facilitating the transfer of gel from aggregates to cracks parallel to unloaded directions, thereby increasing expansion in free directions. Conversely, DEF products, being crystallized and less mobile, struggle to move through cracks once formed. The formation of ettringite is influenced by pressure-induced changes in solubility, pore pressure variations, and crack development, typically resulting in reduced generation of delayed ettringite under load conditions [21].

Durability issues such as DEF or combined ASR and DEF have been reported in concrete infrastructure worldwide [5]. Structural members contain reinforcement that restrains expansion caused by internal swelling reactions. The presence of longitudinal and transverse reinforcement in these members provides better confinement of the concrete core during swelling. However, few comprehensive studies have focused on the structural behavior of DEF-affected reinforced concrete (RC), as most research has examined the mechanical properties and expansion kinetics of plain concrete without confinement. Sanjeewa et al. [24] studied the residual flexural capacity of prestressed concrete beams affected by DEF and combined ASR-DEF through experiments. They observed that the beam stiffness decreased moderately (22% for DEF and 30% for ASR-DEF beams), while the load capacities of damaged beams, despite numerous cracks, were reduced by 16% and 23%, respectively. Overall, a slight reduction in both stiffness and load capacity was noted in RC beams experiencing DEF damage.

Although only a few studies have examined the structural behavior of DEF-damaged concrete, the impact of ASR on the load capacity of RC structures has been more extensively researched. Fan and Hanson [25], Monette et al., and Morenon et al. [26] investigated the flexural performance of ASR-damaged RC beams alongside the mechanical properties of ASR-damaged concrete samples. They found significant degradation in material properties, but no reduction in the flexural capacity of the beams. Additionally, Monette et al. [27] observed that ASR damage can inhibit the development of shear cracks. Ahmed et al. [28] studied both the flexural and shear capacity of ASR-damaged RC beams and discovered a slight increase in both capacities following ASR damage. Similarly, Aryan and Gencturk [29] found through experiments that the shear behavior of beams with ASR damage was comparable to that of undamaged beams. Liu et al. [30] and Karthik et al. [31] reported that the shear stiffness and capacity of D-region reinforced concrete specimens increased slightly when ASR damage was present. The apparent lack of impact on the flexural and shear capacity of ASR-damaged RC beams has been attributed to the chemical prestressing force generated by ASR gel, which can enhance the mechanical properties of cracked concrete [26]. The structural response of RC beams affected by ASR or DEF shows different trends, even though the material-level deterioration in ASR- or DEF-damaged concrete appears similar.

Understanding the residual capacity of an RC structure affected by durability issues is crucial for predicting its long-term performance. While experiments are valuable for studying structural behavior under specific conditions, they cannot easily reveal the internal state of concrete and reinforcement. Numerical simulation, on the other hand, provides an effective method for making such predictions. Among the available simulation tools, discrete methods are particularly suited for modeling concrete affected by durability issues like ASR and DEF, which often cause expansion and cracking. These methods can accurately simulate and analyze cracking behavior [32]. The Lattice Discrete Particle Model (LDPM) is one such discrete method that has been used to simulate durability issues in concrete. Alnaggar et al. [33] and Rezakhani et al. [34] developed LDPM for simulating ASR damage. In their model, aggregates are represented, and a truss network connects aggregate particles. However, mortar is not modeled directly, which can complicate the analysis of cracking behavior. Another discrete method, the Rigid Body Spring Model (RBSM), has been used to simulate durability issues in concrete. Initially proposed by Kawai et al. [35] and further developed by Nagai et al. [36], RBSM is designed for simulating concrete failure at the mesoscale. This method is well-suited for simulating crack propagation within concrete since it accurately models aggregate, mortar, and steel. RBSM can be

categorized into two types based on the simulation scale: the 'aggregate model' and the 'concrete model'. In the aggregate model, aggregate and mortar elements are modeled separately with an element size of 2-3 mm to preserve aggregate shape. This model is commonly used to simulate the behavior of concrete materials [36,37], including ASR, DEF [38,39], frost damage [40–42], and other durability-related phenomena, with local expansion and crack propagation modeled directly at the material scale. In contrast, the concrete model does not separate aggregate and mortar. Instead, it models concrete elements with a larger element size (1-2 cm) and includes reinforcement, making it suitable for simulating the behavior of RC members, as demonstrated in previous research [43–47].

ASR damage has been studied from the material to the member scale using RBSM [38,39,48,49,49–51], while DEF damage has primarily been simulated at the material scale. The bond deterioration in DEF-damaged concrete has also been studied with RBSM, alongside ASR damage cases [50]. Understanding the expansion of concrete DEF under restraint is crucial for further studying DEF-induced damage at the structural scale using 3D RBSM. In this study, DEF expansion under external restraint is simulated using the aggregate model in RBSM. The simulation is based on experimental data. Both macroscopic expansion and anisotropic expansion behavior due to restraint are simulated and discussed. Additionally, not only the surface cracking pattern but also the development of internal cracking is visualized, facilitating further study of DEF damage at the structural level.

## 2. Simulation methodology

### 2.1 Analysis model

The Rigid Body Spring Model (RBSM), originally developed by Kawai et al. [35], is utilized in this study. Nagai et al. [36,37] further advanced simulation systems for concrete failure in both 2D and 3D RBSM. As illustrated in Fig. 1, an RBSM model is discretized into polyhedral rigid elements connected by springs located at the interfaces of each element. These springs include one normal spring and two shear springs. Each element has six degrees of freedom (DOFs): three translational DOFs and three rotational DOFs. The behavior of the elements is governed by the responses of these interface springs. To date, 3D RBSM has been successfully applied to simulate not only the mechanical properties of concrete materials but also the structural responses of reinforced concrete (RC) systems. Additionally, it has been employed to investigate durability issues, including rebar corrosion, alkali-silica reaction (ASR), delayed ettringite formation (DEF), and freezing–thawing cycles (FTCs) [38,39,52–54].

In this study, a model comprising mortar, aggregate, and steel elements is developed to examine the combined behavior of concrete DEF expansion under confinement (Fig. 2). To accurately simulate crack propagation, the mortar and aggregate elements are randomly meshed with a size of approximately 23 mm³. This mesh size has been validated as effective for simulating crack propagation in concrete through various simulation studies [37,39,40,42]. Moreover, the constitutive model employed is specifically designed for this mesh size [37]. The steel elements representing the rebar are modeled at 5 mm intervals along the axial direction, accurately incorporating the ribs to replicate the interaction between the rebar and mortar.

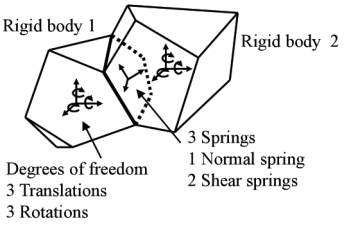


Fig. 1 Element in RBSM

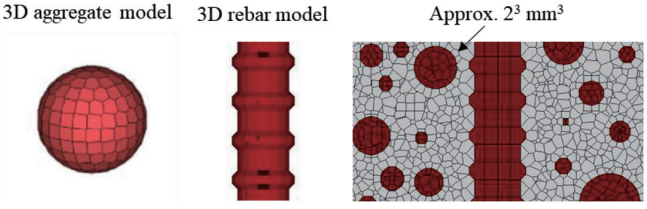


Fig. 2 RC model consisting of mortar, aggregate and steel elements

### 2.2 Constitutive models

The constitutive models, illustrated in Fig. 3, are

detailed in our previous research [38,39,52]. Fig. 3(a) depicts the behavior of the normal and shear springs for both the mortar elements and the mortar-steel interface. For mortar elements, the normal spring exhibits elastic behavior under compression. When the normal spring reaches the tensile strength , fracture occurs between the mortar elements. Following this, the normal stress decreases proportionally to the crack width, defined as the spring elongation. The maximum crack width is set at 0.03 mm. The shear spring follows an elasto-plastic model in regions where the normal springs have not fractured. The value of is determined based on the state of the normal springs and the tensile strength.

The normal and shear springs at the mortar-steel interface follow the same constitutive models shown in Fig. 3(a)-(b). The bond behavior between the rebar and concrete is directly simulated through the interaction between steel and concrete since the ribbed reinforcing bars are accurately modeled in 3D. This approach has successfully simulated macroscopic bond behavior, crack development, and stress concentration on the rebar surface in prior studies [55]. Concrete failure is characterized by sliding and cracking at the meso-scale; therefore, compression yielding is not applied to mortar elements.

For the mortar-aggregate interface, the constitutive models for the normal and shear springs are identical to those of the mortar elements. The criterion for the mortar-aggregate interface follows the model depicted in Fig. 3(c)-(d). These constitutive models are all adapted from our previous research [37].

The behavior of normal springs connecting steel elements is shown in Fig. 3(e), which also follows the constitutive model used in a previous study [47].

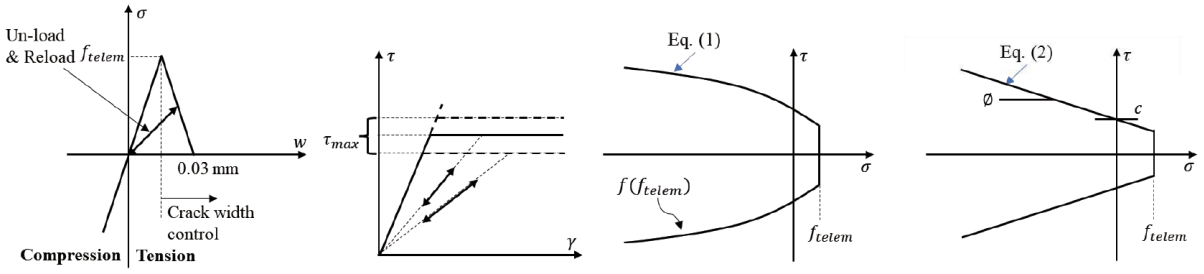


a. Normal spring for mortar b. Shear spring for mortar c. $\tau_{max}$ criteria for mortar d. $\tau_{max}$ criteria for mortar-aggregate interface

e. Normal spring for steel

$$\tau_{max} = \pm\left(0.30 f_{telem}^{2.5}(-\sigma + f_{telem})^{0.4} + 0.15 f_{telem}\right) \quad if(\sigma \le f_{telem}) \quad (1)$$

$$\tau_{max} = \pm(-\sigma tan\emptyset + c) \quad if(\sigma \le f_{telem}) \quad (2)$$

$$\begin{aligned} &\sigma = E_s\varepsilon && if\ (\varepsilon \le \varepsilon_y) \\ &\sigma = f_y && if\ (\varepsilon_y \le \varepsilon \le \varepsilon_{sh}) \\ &\sigma = f_y + \left(1 - e^{\frac{\varepsilon_{sh}-\varepsilon}{k}}\right)(1.01 f_u - f_y) && if\ (\varepsilon > \varepsilon_{sh}) \end{aligned} \quad (3)$$

$\boldsymbol{\sigma}$ and $\boldsymbol{\tau}$: stress of normal and shear springs in MPa;
$\boldsymbol{\varepsilon}$ and $\boldsymbol{\gamma}$: strain of normal and shear springs;
$\boldsymbol{f_{telem}}$: distributed tensile strength of mortar at the mesoscale in MPa;
$\boldsymbol{f_y}$: yield stress of steel springs in MPa;
$\boldsymbol{\varepsilon_y}$: yield strain of steel springs;

Fig. 3 Constitutive model

## 2.3 DEF expansion concept

The DEF expansion model used in this study is based on our previous research [38,39]. Initial DEF expansion strain (mortar expansion) is applied to the normal springs between mortar-mortar elements to simulate the pressure generated by the DEF reaction (Fig. 4(a)). This initial strain is a constant input parameter that accumulates as the simulation progresses, replicating the development of DEF damage without accounting for time dependency. As the curing temperature is significantly higher at the center of the concrete, DEF-induced expansion is more pronounced in this area. To model this behavior, we adopt the concept of an "intensified expansion area" (Fig. 4(b)),

introduced in our earlier work. As shown in Fig. 4(b), the input initial strain decreases linearly from a depth of 25 mm below the model surface, reaching zero at the surface. This "intensified expansion area" approach has been validated as effective in reproducing the surface cracking patterns observed in experiments. In contrast, uniformly applied expansion fails to replicate the typical surface cracking patterns associated with DEF damage [38,39]. However, this assumption is a simplification for simulation purposes. The position and characteristics of the intensified expansion area must be carefully evaluated for practical applications, as real structural conditions are more complex and may differ significantly from the experimental setup.

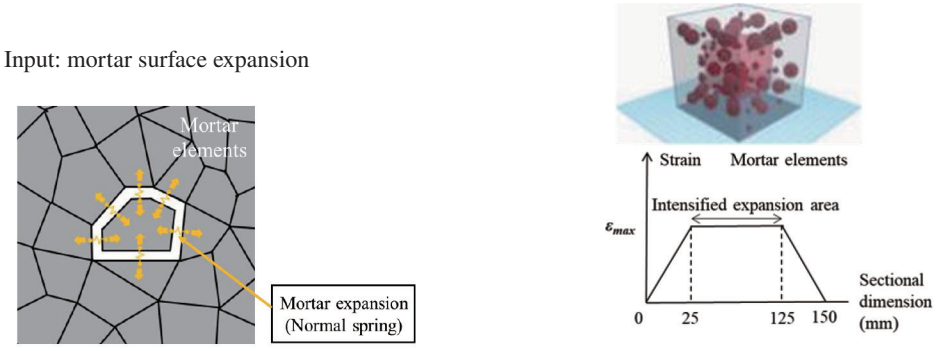


(a) DEF expansion model

(b) Intensified expansion area for DEF damage

Fig. 4 DEF expansion model

## 3. Simulation details

This study simulates the experiment conducted by Kawabata et al. [22], which investigated the expansion of concrete due to DEF damage under restraint. In their experiment, the diameter of the steel rod was considered as a variable. This study mainly discusses the effect of external restraint which is provided by the steel plates, rather than by the longitudinal steel rod connecting them. Therefore, only the model with a steel rod diameter of 13 mm is simulated in this study. Additionally, a concrete model based on the experiment is developed. Table 1 provides the details of the target experiment and the corresponding simulation model IDs. One case with restraint (Model D13), and one case without restraint (Model F) are simulated.

Table 1 Details of target experiment

| Model ID | Dimensions (mm) | Diameter of steel rod (mm) | Thickness of steel plate (mm) | Restraint condition on concrete |
|---|---|---|---|---|
| F | 100 x 100 x 400 | / | / | Free |
| D13 | 100 x 100 x 400 | 13 | 30 | Steel rod and end plates |

### 3.1 Model information

The dimensions of the simulation models are shown in Fig. 5. In model D13, the surface of the steel rod is plain and unbonded to the surrounding mortar elements to replicate the experimental conditions. The aggregate size distribution is determined according to the JSCE standard, with a maximum coarse aggregate size of 20 mm [56]. In all cases, the aggregate percentage is 20%, which is the maximum value that maintains an appropriate mesh shape for the aggregate in the model. This aggregate percentage has also been confirmed as acceptable in previous research [52]. The number of elements in each model is provided in Table 2. As shown in Table 3, the input mesoscopic material properties of the mortar and the aggregate-mortar interface for the simulation are calculated using equations proposed by Nagai et al. [37], based on the water-to-cement ratio from the referenced experiment. The input material properties for the steel elements were not provided in the referenced experiment; therefore, general material properties of steel rods are used in this study.

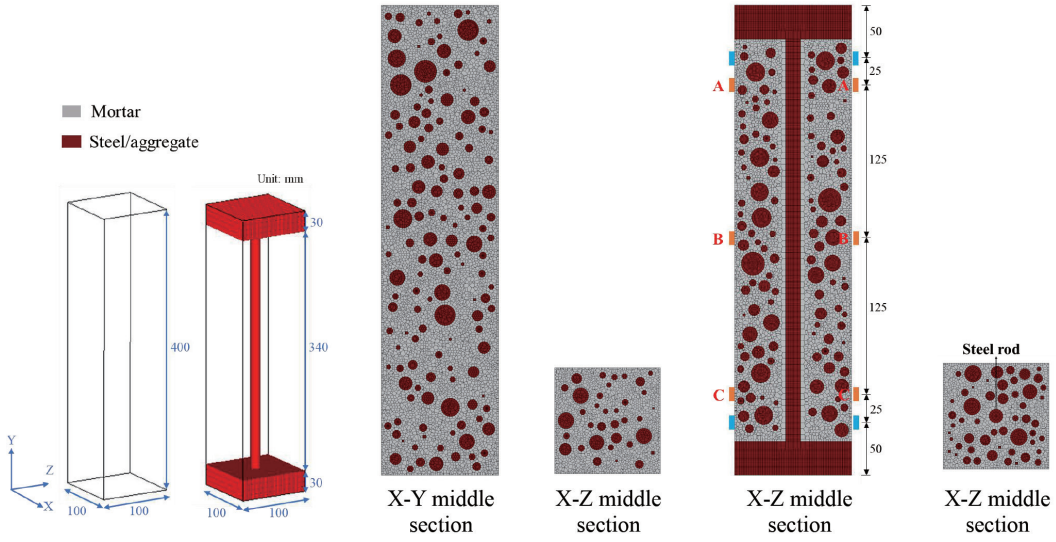


(a) 3D view (b) Model F (c) Model D13

Fig. 5 Dimensions of simulation models

Table 2 Number of elements

| Model ID | Mortar elements | Aggregate elements | Steel elements | Total |
|---|---|---|---|---|
| F | 296683 | 127219 | / | 423902 |
| D13 | 180399 | 145197 | 21952 | 380872 |

Table 3 Input material properties

| Mortar | | Aggregate | Aggregate-mortar interface | Steel | | Steel-mortar interface |
|---|---|---|---|---|---|---|
| Modulus of elasticity (MPa) | Tensile strength (MPa) | Modulus of elasticity (MPa) | Tensile strength (MPa) | Modulus of elasticity (MPa) | Yield strength (MPa) | Tensile strength (MPa) |
| 20760 | 3.2 | 50000 | 1.51 | 201000 | 1300 | 1.6 |

### 3.2 Simulation process

In these simulation models, four points on the top surface are fully fixed during the simulation process to prevent the models from rotating. The DEF expansion model, introduced in Section 2.3, is applied to simulate the DEF expansion behavior. The simulation stops when the longitudinal expansion reaches the value observed in the experiment.

## 4. Simulation results

### 4.1 Macroscopic DEF expansion

The macroscopic DEF expansion in both the longitudinal and transverse directions was recorded in the experiment. As shown in Fig. 5(c), the blue points indicate the locations of the studs used for measuring longitudinal expansion, while the orange points denote the locations for measuring transverse expansion in both the 'F' and 'D13' cases. The transverse expansion at three locations—A, B, and C—was recorded. In the simulation, expansion was applied to the mortar surface to simulate DEF expansion. In the experiment, DEF expansion occurred as a result of a chemical reaction, which is a time-dependent phenomenon with a reaction rate that is difficult to model. Besides, this simulation focuses on the damage caused by the DEF reaction, rather than on the reaction process itself. Therefore, in this study, the time dependency of DEF reaction is not considered. The simulation step was adjusted to the exposure time in experiment based on

macroscopic longitudinal expansion. When a certain value of macroscopic longitudinal expansion was reached in the simulation, the corresponding simulation step was translated into the equivalent exposure time in the experiment (in days).

The average transverse expansion values at locations A, B, and C are used in Fig. 6. As shown in Fig. 6(a), in the experiment, transverse expansion is only slightly higher than longitudinal expansion in the case without any restraint (case F). However, in the simulation, transverse expansion is observed to be lower than longitudinal expansion. The unequal expansion in the longitudinal and transverse directions may be caused by the random size distribution of aggregates.

For the case with restraint by steel plates, as shown in Fig. 6(b), the longitudinal expansion is significantly reduced due to the restraint to approximately 3000μ in the experiment, and the transverse expansion is also reduced compared to the case without any restraint. In the simulation results of model D13, a similar trend is observed, where the longitudinal expansion is restrained by the steel plates from approximately 20000μ to only 3000μ. Regarding the transverse expansion, it exceeds 20000μ, which is an overestimation compared to the experimental results. In the experiment, friction between the concrete and steel plates at the ends of the specimen affects the behavior. Not only is the concrete near the specimen ends laterally restrained, but the central part of the specimen also experiences some degree of lateral restraint. This lateral restraint on DEF expansion appears to be weaker in the simulation.

The simulation results of transverse expansion at different locations are compared in Fig. 7. The transverse expansion at position B is higher than at positions A and C, highlighting the restraining effect of friction between the concrete and steel plates at the ends of the model. The transverse expansion near the ends decreases more due to the stronger restraining effect. The experimental results of the transverse expansion at position B are also presented alongside the simulation results in Fig. 7. It is observed that the simulation results overestimate the transverse expansion recorded in the experiment, indicating weaker lateral restraint on DEF expansion in the simulation.

Overall, the behavior of DEF expansion under restraint is different from ASR expansion case. As above-mentioned, there is evidence from previous experimental work that stress reduces expansion in the restrained direction without a corresponding increase in the unrestrained direction, indicating an absence of expansion transfer [11,21,22]. Researchers pointed out that the DEF product crystallized and less mobile, struggle to move through cracks once formed, therefore, "expansion transfer" cannot be observed in DEF expansion case [11,21,22]. Besides, the formation of ettringite is influenced by pressure-induced changes in solubility. When pore pressure, changes, the generation of DEF products can also be influenced. However, in this study, the crystallized and less mobile nature of DEF products has not been considered. Additionally, the effect of pore pressure change due to external or internal restraint on DEF reaction has not been considered due to the lack of experimental evidence. To quantitatively consider the effect of restraint on the generation of DEF products is difficult. And it will be discussed in the future work together with more detailed experimental works.

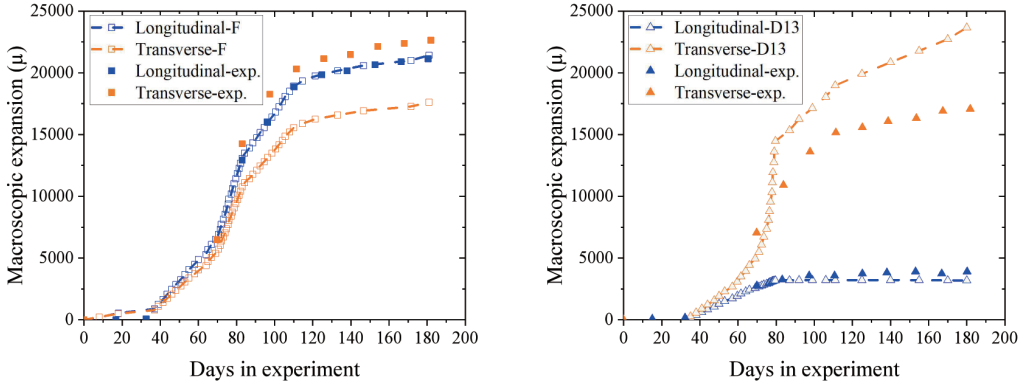


(a) F (b) D13

Fig. 6 Comparison of macroscopic DEF expansion

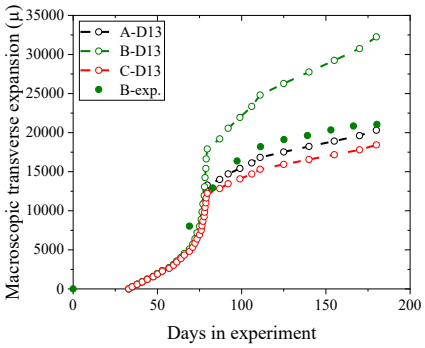


Fig. 7 Comparison of macroscopic transverse DEF expansion

### 4.2 Internal stress and crack development

The stress and crack development during the DEF expansion process for the cases without restraint (F) and with restraint (D13) are shown in Fig. 8. As presented in Fig. 8(a), for the case without restraint (F), the center part of the model is initially in compression because the outer layer experiences less DEF strain. Consequently, the center, which undergoes higher expansion, is confined by the outer layer. As DEF strain increases, gaps between the aggregate and mortar become visible, and large cracks appear near the surface of the model. These cracks widen as DEF damage progresses. On the model surface, random visible cracks occur when the longitudinal DEF expansion reaches 5,000μ. As the DEF expansion continues, more cracks form and develop.

As shown in Fig. 9(b), for the case with restraint (D13), the center part of the model is initially in compression, similar to the case without restraint (F). The steel rod experiences tension due to concrete expansion. As the DEF strain increases, gaps can be observed at the interfaces between the steel-mortar and the aggregate-mortar. When macroscopic longitudinal expansion reaches 3200 μ, the gap between the steel and surrounding mortar elements becomes quite large. Additionally, the gaps at the aggregate surface become larger and tend to connect longitudinally due to the restraint in that direction. Regarding surface cracking, large longitudinal cracks appear first and develop due to the restraining stress, while transverse cracks form later and are narrower. Overall, the development of both internal and surface cracking is significantly influenced by the restraint.

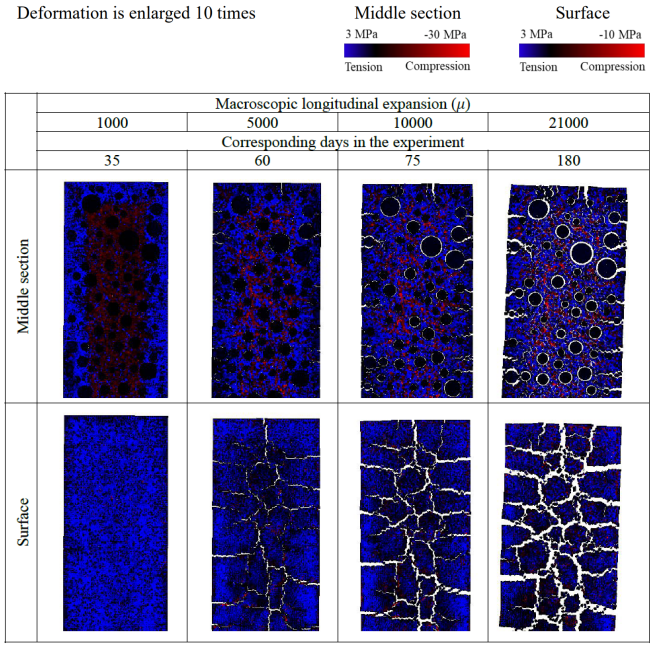


(a)Without restraint (F)

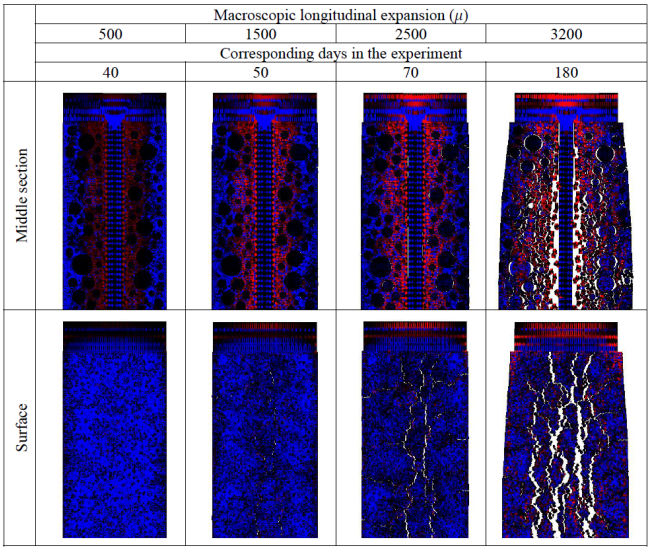


(b) With restraint (D13)

Fig. 8 Stress and crack development in the models

The comparison of internal stress conditions for cases F and D13 is presented in Figs. 9 and 10, respectively. In these figures, fluorescence highlights the cracks observed in the experiment. For case without restraint (F) (Fig. 9), in the experiment, cracks are distributed along the aggregate surface, and some can be seen near the surface in both the X-Y and X-Z center

sections. Similarly, in the simulation results, large gaps are observed at the aggregate surface and near the surface of the model, showing a trend consistent with the experimental observations.

As shown in Fig. 10, in the experiment, cracks are visible at the steel rod and aggregate surfaces, as well as near the surface of the concrete specimen in both the X-Y and X-Z center sections. In the simulation results for case D13, large gaps are similarly observed at the steel rod and aggregate surfaces and near the model's surface, showing that internal cracking conditions are well simulated by the 3D RBSM.

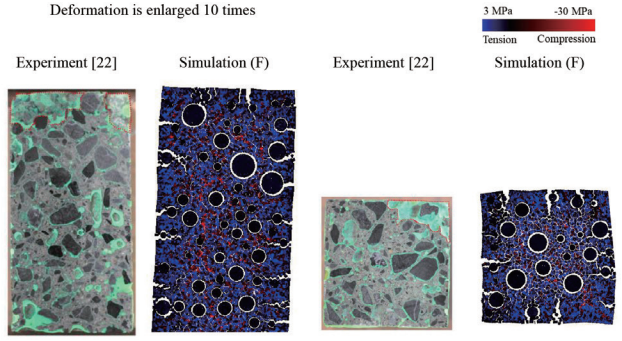


(a) X-Y center section (b) X-Z center section

Fig. 9 Comparison of internal stress condition for case without restraint

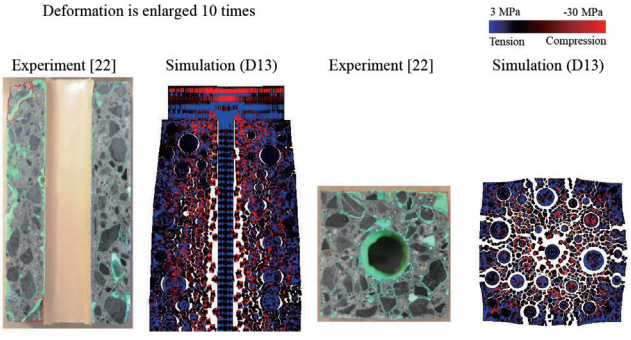


(a) X-Y center section (b) X-Z center section

Fig. 10 Comparison of internal stress condition for case with restraint

### 4.3 Surface cracking pattern

The surface cracking patterns observed in the experiment and simulation are shown together in Fig. 11. For the simulation results, the deformation has been enlarged by 10 times. For the case without restraint (F), both the experiment and simulation display a random cracking pattern on the surface. However, there is a small difference: cracks near the edges of the specimen are wider in the experiment, which differs from the simulation results. In the restrained case, the experimental results show that cracks tend to be distributed longitudinally, with some transverse cracks also visible. In the simulation results for D13, large longitudinal cracks are observed in the central part of the surface, along with narrower transverse cracks. The RBSM simulation results show more concentrated cracks in the restrained (longitudinal) direction. Although the simulated surface cracking pattern is not entirely identical to that observed in the experiment, the overall cracking trend is well captured in the simulation.

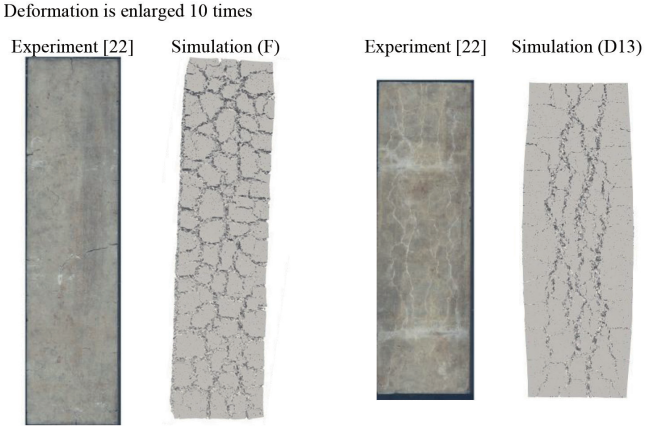


(a) Without restraint (b) With restraint

Fig. 11 Surface cracking pattern

### 4.4 Strain development on steel rod

The strain in the central section of the steel rod, obtained from the simulation, and the macroscopic longitudinal expansion of the concrete surface are shown in Fig. 12. In simulation, when the DEF expansion is relatively small, the strain on the steel rod is nearly the same as the longitudinal expansion of the concrete surface. As the DEF expansion increases (after 70 days in the experiment), a gap begins to form between the steel rod and the surrounding mortar (seeing Fig. 8(b)). Subsequently, the concrete near the model surface moves out of the restraint zone of the steel plate. Due to the reduced restraint in the surface area compared to the concrete near the steel rod, the

macroscopic longitudinal expansion of the concrete surface becomes slightly larger than the strain on the steel rod. This outcome is considered reasonable.

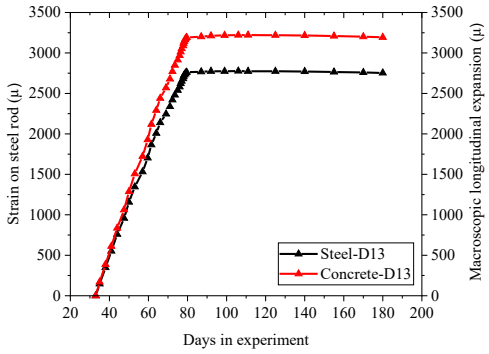


Fig. 12 Strain on steel rod and concrete

## 5. Conclusions

This paper applies the 3D RBSM model to simulate concrete DEF expansion under restrained conditions. It not only simulates the macroscopic expansion behavior but also visualizes internal stress and crack development. The following conclusions can be drawn from the simulation:

(1)The 3D RBSM effectively simulates the DEF expansion behavior of unrestrained concrete. It accurately replicates isotropic expansion behavior and random surface cracking patterns, while also visualizing internal stress and crack development.

(2)DEF expansion under the restraint of steel plates has been simulated using RBSM. While it can simulate anisotropic expansion behavior, the transverse expansion is significantly overestimated. The lateral restraint on DEF expansion appears weaker in the simulation.

(3)Regarding the internal cracking pattern, the RBSM model captures internal cracking well. For surface cracking, the RBSM simulation results show more concentrated cracks in the restrained (longitudinal) direction. In experiments, although large longitudinal cracks are present, transverse cracks are also observed. However, the simulation effectively captures the general trend of surface cracking.

(4)The DEF expansion model used in the simulation does not account for the crystallized and less mobile nature of DEF products. Additionally, the effect of pore pressure changes, due to external or internal restraint, on the DEF reaction has not been considered, as this is difficult to study quantitatively. This aspect will be addressed in future work, along with more detailed experimental studies.

## Declaration of competing interest

**Jie Luo:** Data curation, Investigation, Writing – original draft. **Shingo Asamoto:** Supervision, Writing – review & editing. **Kohei Nagai:** Conceptualization, Funding acquisition, Methodology, Supervision, Writing – review & editing.

## Acknowledgements

This work was supported by JSPS KAKENHI Grant Numbers JP22H00224.

## References

[1] Thomas, M.; Folliard, K.; Drimalas, T.; Ramlochan, T. (2008) "Diagnosing delayed ettringite formation in concrete structures," Cement and Concrete Research, 38, PP. 841 ~847. https://doi.org/10.1016/j.cemconres.2008.01.003

[2] Joshi, N.R.; Matsumoto, A.; Asamoto, S.; Miura, T; Kawabata, Y. (2022) "Investigation of the mechanical behaviour of concrete with severe delayed ettringite formation expansion focusing on internal damage propagation under various compressive loading patterns," Cement and Concrete Composites, 128, pp. 104433. https://doi.org/10.1016/j.cemconcomp.2022.104433

[3] Karthik, M.M.; Mander, J.B.; Hurlebaus, S. (2016) "Deterioration data of a large-scale reinforced concrete specimen with severe ASR/DEF deterioration," Construction and Building Materials, 124, pp. 20–30. https://doi.

org/10.1016/j.conbuildmat.2016.07.072

[4] Larson, N.A.; Bayrak, O.; James, J.O.; Jirsa, O. (2012) "Effects of alkali-silica reaction and delayed ettringite formation on anchorage of prestressing strands in trapezoidal box beams with dapped ends," PCI Journal, 57, pp. 119~131. https://doi.org/10.15554/pcij.06012012.119.131

[5] Taylor, H.F.W.; Famy, C.; Scrivener, K.L. (2001) "Delayed ettringite formation," Cement and Concrete Research, 31, pp. 683~693. https://doi.org/10.1016/S0008-8846(01)00466-5

[6] Flatt, R.J.; Scherer, G.W. (2008) "Thermodynamics of crystallization stresses in DEF," Cement and Concrete Research, 38, pp. 325~336. https://doi.org/10.1016/j.cemconres.2007.10.002

[7] Sellier, A.; Sellier, S (2018) "Chemical modelling of Delayed Ettringite Formation for assessment of affected concrete structures," Cement and Concrete Research, 108, pp. 72~86. https://doi.org/10.1016/j.cemconres.2018.03.006

[8] Martin, R.P.; Omikrine Metalssi, O.; Toutlemonde, F. (2013) "Importance of considering the coupling between transfer properties, alkali leaching and expansion in the modelling of concrete beams affected by internal swelling reactions," Construction and Building Materials, 49, pp. 23~30. https://doi.org/10.1016/j.conbuildmat.2013.08.008

[9] Omikrine Metalssi, O.; Kchakech, B.; Kchakech, S.; Godart, B. (2016) "A New Model for the Analysis of the Structural/mechanical Performance of Concrete Structures Affected by DEF - Case Study of an Existing Viaduct," Structural Concrete.

[10] Jones, A.E.K.; Clark, L.A. (1996) "The effects of restraint on ASR expansion of reinforced concrete," Magazine of Concrete Research, 48, pp. 1~13. https://doi.org/10.1680/macr.1996.48.174.1

[11] Multon, S.; Toutlemonde, F. (2006) "Effect of applied stresses on alkali–silica reaction-induced expansions," Cement and Concrete Research, 36, pp. 912~920. https://doi.org/10.1016/j.cemconres.2005.11.012

[12] Dunant, C.F.; Dunant, K.L. (2024) "Effects of uniaxial stress on alkali–silica reaction induced expansion of concrete," Cement and Concrete Research, 42, pp. 567~576. https://doi.org/10.1016/j.cemconres.2011.12.004

[13] Berra, M.; Faggiani, G.; Faggiani, T.; Paolini, A.E. (2010) "Influence of stress restraint on the expansive behaviour of concrete affected by alkali-silica reaction," Cement and Concrete Research, 40, pp. 1403~1409. https://doi.org/10.1016/j.cemconres.2010.05.002

[14] Kagimoto, H.; Yasuda, Y.; Kawamura, M. (2014) "ASR expansion, expansive pressure and cracking in concrete prisms under various degrees of restraint," Cement and Concrete Research, 59, pp. 1~15. https://doi.org/10.1016/j.cemconres.2014.01.018

[15] Gautam, B.P.; Panesar, D.K.; Panesar, S.A.; Vecchio, F.J. (2017) "Multiaxial Expansion-Stress Relationship for Alkali Silica Reaction-Affected Concrete," ACI Materials Journal, 114, pp. 171~182. https://doi.org/10.14359/51689490

[16] Hayes, N.W.; Gui, Q.; Abd-Elssamd, A.; Pape, Y.L.; Giorla, A.B.; Pape, S.L.; Giannini, E.R.; Ma, Z.J. (2018) "Monitoring Alkali-Silica Reaction Significance in Nuclear Concrete Structural Members," Journal of Advanced Concrete Technology, 16, pp. 179~190. https://doi.org/10.3151/jact.16.179

[17] Liaudat, J.; Carol, I.; López, C.M.; Saouma, V.E. (2018) "ASR expansions in concrete under triaxial confinement," Cement and Concrete Composites, 86, pp. 160~170. https://doi.org/10.1016/j.cemconcomp.2017.10.010

[18] Kongshaug, S.S.; Oseland, O.; Oseland, T.; Hendriks, M.A.N.; Hendriks, E.; Markeset, G. (2020) "Experimental investigation of ASR-affected concrete – The influence of uniaxial loading on the evolution of mechanical properties, expansion and damage indices," Construction and Building Materials, 245, pp. 118384. https://doi.org/10.1016/j.conbuildmat.2020.118384

[19] Mohammed, T.U.; Hamada, H.; Hamada, T.

(2003) "Relation between Strain on Surface and Strain over Embedded Steel Bars in ASR Affected Concrte Members," Journal of Advanced Concrete Technology, 1.

[20] Morenon, P.; Morenon, S.; Sellier, A.; Sellier, E.; Hamon, F.; Hamon, E. (2017) "Impact of stresses and restraints on ASR expansion," Construction and Building Materials, 140, pp. 58~74. https://doi.org/10.1016/j.conbuildmat.2017.02.067

[21] Bouzabata, H.; Multon, S.; Sellier, A.; Houari, H. (2012) "Effects of restraint on expansion due to delayed ettringite formation," Cement and Concrete Research, 42 (2012) 1024–1031. https://doi.org/10.1016/j.cemconres.2012.04.001

[22] Y. Kawabata, N. Ueda, T. Miura, S. Multon, The influence of restraint on the expansion of concrete due to delayed ettringite formation, Cement and Concrete Composites 121, pp. 104062. https://doi.org/10.1016/j.cemconcomp.2021.104062

[23] Thiebaut, Y.; Multon, S.; Multon, A.; Lacarrière, L; Lacarrière, L.; Belili, D.; Linger, L.; Cussigh, F.; Hadji, S. (2018) "Effects of stress on concrete expansion due to delayed ettringite formation," Construction and Building Materials, 183, pp. 626~641. https://doi.org/10.1016/j.conbuildmat.2018.06.172

[24] Sanjeewa, H.V.A.N.; Matsumoto, A.; Asamoto, S.; Asamoto, R.-P.; Toutlemonde, F. (2024) "Experimental study on flexural behaviour of DEF–ASR-affected prestressed concrete beams," Engineering Structures, 319, pp. 118835. https://doi.org/10.1016/j.engstruct.2024.118835

[25] Fan, S.; Fan, J.M. (1998) Effect of Alkali Silica Reaction Expansion and Cracking on Structural Behavior of Reinforced Concrete Beams, ACI Structural Journal, 95, pp. 498~505. https://doi.org/10.14359/564

[26] Morenon, P.; Multon, S.; Sellier, A.; Grimal, E.; Hamon, F.; Hamon, P. "Flexural performance of reinforced concrete beams damaged by Alkali-Silica Reaction," Cement and Concrete Composites, 104, pp. 103412. https://doi.org/10.1016/j.cemconcomp.2019.103412

[27] Monette, L.J.; Monette, N.J.; Grattan-Bellew, P.E. (2002) "Residual Strength of Reinforced Concrete Beams Damaged by Alkali-Silica Reaction—Examination of Damage Rating Index Method," ACI Materials Journal, 99, pp. 42~50. https://doi.org/10.14359/11315

[28] Ahmed, T., Burley, E., & Rigden, S. (1998) "The State and Fatigue Strength of Reinforced Concrete Beams Affected by Alkali-Silica Reaction," ACI Materials Journal, 95(4), pp. 376~388. https://doi.org/10.14359/380

[29] Aryan, H., & Gencturk, B. (2021) "Influence of alkali-silica reaction on the shear capacity of reinforced concrete beams with minimum transverse reinforcement," Engineering Structures, 235, pp. 112020. https://doi.org/10.1016/j.engstruct.2021.112020

[30] Liu, S.-H., Bracci, J. M., Mander, J. B., & Hurlebaus, S. (2017) "Performance of D-Regions Affected by Alkali-Silica Reaction: Experimental and Analytical Study," Journal of Structural Engineering, 143(9), pp. 04017109. https://doi.org/10.1061/(ASCE)ST.1943-541X.0001847

[31] Karthik, M. M., Mander, J. B., & Hurlebaus, S. (2018) "Experimental Behavior of Large Reinforced Concrete Specimen with Heavy ASR and DEF Deterioration," Journal of Structural Engineering, 144(8), pp. 04018110. https://doi.org/10.1061/(ASCE)ST.1943-541X.0002102

[32] Bolander, J. E., Eliáš, J., Cusatis, G., & Nagai, K. (2021) "Discrete mechanical models of concrete fracture," Engineering Fracture Mechanics, 257, pp. 108030. https://doi.org/10.1016/j.engfracmech.2021.108030

[33] Alnaggar, M., Cusatis, G., & Luzio, G. D. (2013) "Lattice Discrete Particle Modeling (LDPM) of Alkali Silica Reaction (ASR) deterioration of concrete structures," Cement and Concrete Composites, 41, pp. 45~59. https://doi.org/10.1016/j.cemconcomp.2013.04.015

[34] Rezakhani, R., Alnaggar, M., & Cusatis, G. (2019) "Multiscale Homogenization Analysis of Alkali–Silica Reaction (ASR) Effect in Concrete," Engineering, 5(6), pp. 1139~1154. https://doi.org/10.1016/j.eng.2019.02.007

[35] Kawai, T. (1978) "New discrete models and their application to seismic response analysis of structures," Nuclear Engineering and Design, 48(1), pp. 207~229. https://doi.org/10.1016/0029-5493(78)90217-0

[36] Nagai, K., Sato, Y., & Ueda, T. (2004) "Mesoscopic Simulation of Failure of Mortar and Concrete by 2D RBSM," Journal of Advanced Concrete Technology, 2(3), pp. 359~374. https://doi.org/10.3151/jact.2.359

[37] Nagai, K., Sato, Y., & Ueda, T. (2005) "Mesoscopic Simulation of Failure of Mortar and Concrete by 3D RBSM," Journal of Advanced Concrete Technology, 3(3), pp. 385~402. https://doi.org/10.3151/jact.3.385

[38] Wang, Y., Jiradilok, P., Nagai, K., & Asamoto, S. (2020) "A mesoscale discrete model for mechanical performance of concrete damaged by coupled ASR and DEF," Engineering Fracture Mechanics, 232, pp. 107055. https://doi.org/10.1016/j.engfracmech.2020.107055

[39] Wang, Y., Meng, Y., Jiradilok, P., Matsumoto, K., Nagai, K., & Asamoto, S. (2019) "Expansive cracking and compressive failure simulations of ASR and DEF damaged concrete using a mesoscale discrete model," Cement and Concrete Composites, 104, pp. 103404. https://doi.org/10.1016/j.cemconcomp.2019.103404

[40] Gong, F., Ueda, T., Wang, Y., Zhang, D., & Wang, Z. (2017) "Mesoscale simulation of fatigue behavior of concrete materials damaged by freeze-thaw cycles," Construction and Building Materials, 144, pp. 702~716. https://doi.org/10.1016/j.conbuildmat.2017.03.207

[41] Ueda, T., Hasan, M., Nagai, K., Sato, Y., & Wang, L. (2009) "Mesoscale Simulation of Influence of Frost Damage on Mechanical Properties of Concrete," Journal of Materials in Civil Engineering, 21(6), pp. 244~252. https://doi.org/10.1061/(ASCE)0899-1561(2009)21:6(244)

[42] Gong, F., Ueda, T., & Zhang, D. (2018) "Two-dimensional rigid body spring method based micro-mesoscale study of mechanical strengthening/damaging effects to concrete by frost action," Structural Concrete, 19(4), pp. 1131~1145. https://doi.org/10.1002/suco.201700200

[43] Avadh, K., Jiradilok, P., Bolander, J. E., & Nagai, K. (2021) "Mesoscale simulation of pull-out performance for corroded reinforcement with stirrup confinement in concrete by 3D RBSM," Cement and Concrete Composites, 116, pp. 103895. https://doi.org/10.1016/j.cemconcomp.2020.103895

[44] Avadh, K., Jiradilok, P., Bolander, J. E., & Nagai, K. (2021) "Direct observation of the local bond behavior between corroded reinforcing bars and concrete using digital image correlation," Cement and Concrete Composites, 123, pp. 104180. https://doi.org/10.1016/j.cemconcomp.2021.104180

[45] Avadh, K., Jiradilok, P., Bolander, J. E., & Nagai, K. (2022) "3D mesoscale simulation of the influence of corrosion on loss of tension stiffening in reinforced concrete," Construction and Building Materials, 339, pp. 127684. https://doi.org/10.1016/j.conbuildmat.2022.127684

[46] Hayashi, D., Nagai, K., & Eddy, L. (2017) "Mesoscale Analysis of RC Anchorage Performance in Multidirectional Reinforcement Using a Three-Dimensional Discrete Model," Journal of Structural Engineering, 143(7), pp. 04017059. https://doi.org/10.1061/(ASCE)ST.1943-541X.0001780

[47] Eddy, L., Jiradilok, P., Matsumoto, K., & Nagai, K. (2020) "Analytical investigation of the role of reinforcement in perpendicular beams of beam-column knee joints by 3D meso-scale model," Engineering Structures, 210, pp. 110347. https://doi.org/10.1016/j.engstruct.2020.110347

[48] Luo, J., Asamoto, S., & Nagai, K. (2023) "Mesoscale simulation of compression-induced cracking and failure of ASR-damaged concrete with stirrup confinement," Engineering Fracture Mechanics, 277, pp. 108977. https://doi.org/10.1016/j.engfracmech.2022.108977

[49] Luo, J., & Nagai, K. (2023) "Investigating equivalency of different element models in discrete mesoscale analysis of ASR-damaged concrete," Construction and Building Materials, 408, pp. 133755. https://doi.org/10.1016/

j.conbuildmat.2023.133755

[50] Luo, J., Asamoto, S., & Nagai, K. (2022) "An analytical investigation of bond deterioration between rebar and ASR/DEF-damaged concrete with and without stirrup confinement using 3D RBSM," Construction and Building Materials, 351, pp. 128923. https://doi.org/10.1016/j.conbuildmat.2022.128923

[51] Luo, J., & Nagai, K. (2024) "Investigating the flexural behavior of ASR-damaged RC beam through internal stress and cracking development using 3D Rigid Body Spring Model," Structural Concrete, 25(6), pp. 4623~4638. https://doi.org/10.1002/suco.202400255

[52] Luo, J., Wang, Y., Asamoto, S., & Nagai, K. (2022) "Mesoscopic simulation of crack propagation and bond behavior in ASR damaged concrete with internal/external restraint by 3D RBSM," Cement and Concrete Composites, 129, pp. 104488. https://doi.org/10.1016/j.cemconcomp.2022.104488

[53] Wang, Z., Gong, F., & Ueda, T. (2021) "Modeling and Simulation on Static and Fatigue Behaviors of Intact and Frost Damaged Concrete with Ice-strengthening Effects," Journal of Advanced Concrete Technology, 19(4), pp. 346~358. https://doi.org/10.3151/jact.19.346

[54] Wang, Z., Zhang, D., Gong, F., Mehrpay, S., & Ueda, T. (2021) "Multiscale Modeling and Simulation of Ice-Strengthening Effects in Mesocracks of Saturated Frost-Damaged Concrete under Freezing Temperature," Journal of Materials in Civil Engineering, 33(2), pp. 04020443. https://doi.org/10.1061/(ASCE)MT.1943-5533.0003450

[55] Eddy, L., Matsumoto, K., Nagai, K., & Wang, Z. (2018) Investigation of effect of local bond model on crack propagation in RC using 3D RBSM, In Computational Modelling of Concrete Structures. CRC Press.

[56] JSCE. (2005) Standard Specification for Concrete Structures-2002 'material and Construction' 6.2.5.3 Grading, JSCE Guidelines for Concrete, Japan Society of Civil Engineers.